

# Surface-emitting fiber lasers

Ofer Shapira\*, Ken Kuriki\*, Nicholas D. Orf, Ayman F. Abouraddy, Gilles Benoit, Jean F. Viens, Alejandro Rodriguez, Mihai Ibanescu, John D. Joannopoulos, and Yoel Fink

Research Laboratory of Electronics, Massachusetts Institute of Technology, Cambridge, Massachusetts 02139, USA

\*These authors contributed equally

[yoel@mit.edu](mailto:yoel@mit.edu)

Megan M. Brewster

Department of Material Science and Engineering, University of Washington, Seattle, Washington 98195, USA

**Abstract:** All fiber lasers to date emit radiation only along the fiber axis. Here a fiber that exhibits laser emission that is radially directed from its circumferential surface is demonstrated. A unique and controlled azimuthally anisotropic optical wave front results from the interplay between a cylindrical photonic bandgap fiber resonator, anisotropic organic dye gain, and a linearly polarized axial pump. Low threshold (86nJ) lasing at nine different wavelengths is demonstrated throughout the visible and near-infrared spectra. We also report the experimental realization of unprecedented layer thicknesses of 29.5 nm maintained throughout meter-long fibers. Such a device may have interesting medical applications ranging from photodynamic therapy to in vivo molecular imaging, as well as textile fabric displays.

©2006 Optical Society of America

OCIS codes: (140.3510) Lasers, fiber; (140.3410) Laser resonators; (140.2050) Dye lasers

---

## References and Links

1. M. J. F. Digonnet, *Rare-Earth-Doped Fiber Lasers and Amplifiers* (Marcel Dekker, Inc., Stanford, California, 1993).
2. W. J. Wadsworth, J. C. Knight, W. H. Reeves, P. S. Russell, and J. Arriaga, "Yb<sup>3+</sup>-doped photonic crystal fiber laser," *Elect. Lett.* **36**, 1452-1454 (2000).
3. A. Argyros, N. Issa, I. Bassett, and M. A. van Eijkelenborg, "Microstructured optical fiber for single-polarization air guidance," *Opt. Lett.* **29**, 20-22 (2004).
4. P. Yeh, A. Yariv, and E. Marom, "Theory of Bragg fiber," *J. Opt. Soc. Am.* **68**, 1196-1201 (1978).
5. R. M. Verdaasdonk, and C. F. P. van Swol "Laser light delivery systems for medical applications," *Phys. Med. Biol.* **42** 869-887 (1997).
6. V. Ntziachristos C. Bremer, and R. Weissleder "Fluorescence imaging with near-infrared light: new technological advances that enable in vivo molecular imaging," *Eur. Radiol.* **13**, 195-208 (2003).
7. V. Koncar, "Optical fiber fabric displays," *Opt. Photon. News* **16**, 40-44 (2005).
8. B. Temelkuran, S. D. Hart, G. Benoit, J. D. Joannopoulos, and Y. Fink, "Wavelength-scalable hollow optical fibers with large photonic bandgaps for CO<sub>2</sub> laser transmission," *Nature* **420**, 650-653 (2002).
9. S. D. Hart, G. R. Maskaly, B. Temelkuran, P. H. Pridaux, J. D. Joannopoulos, and Y. Fink, "External reflection from omnidirectional dielectric mirror fibers," *Science* **296**, 510-513 (2002).
10. K. Kuriki, O. Shapira, S. D. Hart, G. Benoit, Y. Kuriki, J. F. Viens, M. Bayindir, J. D. Joannopoulos, and Y. Fink, "Hollow multilayer photonic bandgap fibers for NIR applications," *Opt. Express.* **12**, 1510-1517 (2004).
11. K. Kuriki, et al., Research Laboratory of Electronics, Massachusetts Institute of Technology, Cambridge, Massachusetts 02139, USA, are preparing a manuscript to be called "Hollow-core Photonic Band gap Fibers for High-power Ultraviolet Transmission."
12. F. P. Schafer, *Dye lasers* (Springer-Verlag, Berlin, 1989).
13. T. Erdogan, O. King, G. W. Wicks, D. G. Hall, E. H. Anderson, M. J. Rooks, "Circularly symmetrical operation of a concentric-circle-grating, surface-emitting, AlGaAs/GaAs quantum-well semiconductor-laser. *App. Phys. Lett.* **60**, 1921-1923 (1992).
14. J. Scheuer, W. M. J. Green, and A. Yariv, "Annular Bragg Resonators: Beyond the limits of total internal reflection," *Photon. Spectra* **39**, 64 (2005).

## 1. Introduction

The great variety of optical cavities and their coupling to gain media has made lasers pervasive in science and technology. In particular, fiber lasers have recently been the focus of much interest [1-3]. A common feature of all fiber lasers is the emission along the fiber axis from an area that is small when compared to the total cavity surface and with nearly planar wave front. Here we report on the design, fabrication and characterization of a photonic band gap fiber laser that emits radiation in the plane transverse to the fiber axis from an extended surface area. Furthermore, the unique wave front is azimuthally anisotropic with a radiation pattern resembles an optical dipole. This is due to the interaction between a cylindrical resonator, anisotropic gain, and a linearly polarized axial pump beam. The cylindrical fiber-cavity structure consists of a hollow-core multilayer [4] photonic band gap fiber, and an organic dye gain medium that is introduced into the core. The complete photonic band gap provides the longitudinal confinement of the higher-frequency optical pump and at the same allows light to travel along the fiber at steep angles (with respect to the fiber axis) not afforded by conventional index-guiding fibers. Lasing at 9 different wavelengths is demonstrated throughout the visible and near-infrared spectra. We also report the experimental realization of unprecedented layer thicknesses of 29.5 nm maintained throughout meter-long fibers. Such a device may have interesting medical applications ranging from photodynamic therapy [5] to in vivo molecular imaging [6], as well as textile fabric displays [7].

## 2. Fiber laser structure

The surface-emitting fiber laser structure and pumping arrangement are shown schematically in Fig. 1. The structure comprises a gain medium in the core surrounded by a photonic band gap (PBG) structure [8-11] made of 58 layers of a wide mobility gap amorphous semiconductor,  $As_2S_3$ , alternating with a high glass-transition temperature polymer, poly(etherimide) (PEI). A scanning electron microscope micrograph of the multilayer structure [Fig. 2(a)] demonstrates the uniformity of the layer thicknesses throughout the fiber. The individual layer thicknesses of  $As_2S_3$  and PEI are 59 nm and 89 nm, respectively, and the structure is terminated by a 29.5-nm thick layer of  $As_2S_3$  to eliminate surface modes. The gain medium is pumped axially while the resonant cavity provided by the PBG ensures laser emission in the radial direction. The PBG structure performs a dual role enabled by the characteristic shift of the band edges to higher frequencies with increase in wave vector as depicted in Fig. 2(b). The normal-incidence band gap, defined for axial wave vector  $k=0$  (region A), provides the optical feedback necessary for emitting laser light from the whole surface area in the radial direction. Concurrently, the blue-shifted band gap having axial wave vectors near the light line (region B) is responsible for guiding the pump frequency.

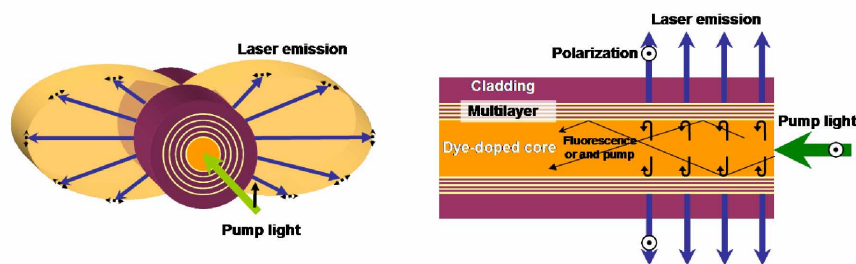


Fig. 1. Photonic band gap fiber laser. The fiber laser emits light in the transverse direction (propagation and polarization vectors shown as solid arrows and dashed lines, respectively) having a dipole-like wave front from an extended length of the fiber.

While different types of gain media may be used in conjunction with the fiber, for convenience we chose an organic laser dye [12] incorporated into a copolymer matrix. The upper inset in Fig. 2(a) is a fluorescence micrograph of the fiber cross section (see Appendix A). An organic dye, LDS698, having a fluorescence peak at 645 nm was dispersed in a copolymer and inserted into the otherwise hollow core of a PBG fiber. Since the normal-incidence PBG is 26% of its centre-frequency, it encompasses the entire fluorescence spectrum as shown in Fig. 2(c) (see Appendix B). This same fiber supports the propagation of a pulsed optical pump at 532 nm traveling through the fiber core.

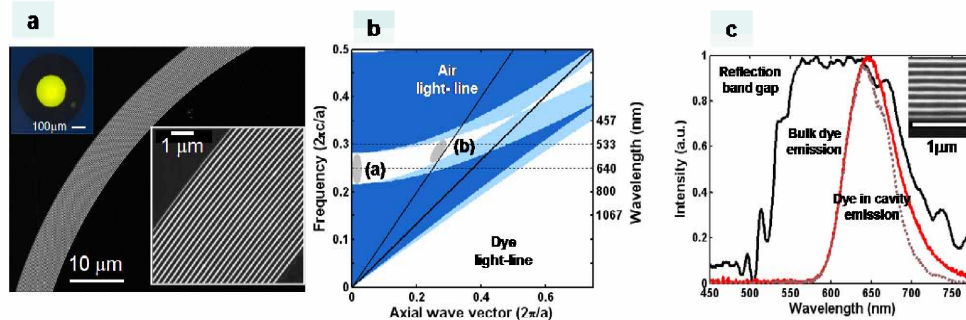


Fig. 2. Structure of the fiber laser cavity. (a), Cross-sectional SEM micrographs of the PBG multilayer structure at various magnifications. The PEI in the cladding and the layers appears black, and the  $As_2S_3$  layers white. The PEI and  $As_2S_3$  layers are 89 nm and 59 nm thick (except for the first and last  $As_2S_3$  layers which are 29.5 nm thick; the first layer is not visible). The top left inset shows a cross-sectional fluorescence micrograph of the full cross-section of a PBG fiber with an R590 organic dye in the core and enveloped by a thick PEI protective cladding. (b), Projected band structure of a one dimensional photonic crystal consisting of alternating layers of  $As_2S_3$  and PEI. Transverse-electric (TE) and transverse-magnetic (TM) propagating modes are in dark and light blue, respectively; evanescent modes are in white. Light incident normally to the structure ( $k=0$ ) and axially propagating modes through the hollow core are shown as regions A and B, respectively. (c), Measured reflection band gap centered around 620nm (see 'Optical characterization' in methods) in black; fluorescence spectrum of LDS698 (500 ppm concentration) in red; and calculated dye-in-cavity emission obtained by multiplying the last two, dashed line.

### 3. Optical properties

We observe broad fluorescence emission from the above described fiber laser at pump-pulse energies lower than the 86 nJ threshold, while radially directed lasing occurs with sharp peaks at 652 nm above threshold [Fig. 3(a)]. To confirm that the emitted radiation is indeed laser light and not amplified spontaneous emission, we show in Fig. 3a the emission spectra of the fiber for three different pump energies: below (A), near (B) and above (C) threshold. The lasing threshold occurs at pump energies of 86 nJ and 110 nJ for dye concentration of 500 ppm and 50ppm, respectively. The dependence of the emission bandwidth (Fig. 3a inset) and energy [Fig. 3(b)] on the pump energy for both 500 ppm and 50 ppm dye concentrations are shown. Both clearly demonstrate laser thresholds. The slope efficiencies are 37.5% and 16.5% for the 500 ppm and 50 ppm concentrations, respectively.

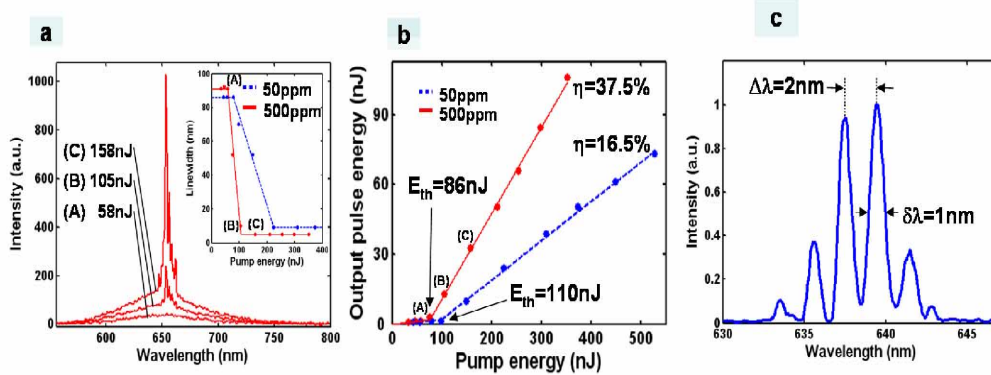


Fig. 3. Lasing characteristics of an LDS698-doped PBG fiber. a, Emission spectra of the fiber laser for a dye concentration of 500 ppm and pump energy below threshold (A),  $1.2E_{th}$  (B) and  $1.8E_{th}$  (C), where  $E_{th}$  is the lasing threshold energy. Inset shows the spectral full-width at half-maximum as a function of input energy for 500 ppm (red line) and 50 ppm (dashed blue). b, Dependence of the laser energy on the pump energy showing threshold values of  $E_{th} = 86$  nJ and  $E_{th} = 100$  nJ for the 500 ppm and 50 ppm, respectively. c, High resolution spectral measurement reveals mode spacing of 2 nm and quality factor of 640.

The PBG fiber (core diameter  $d_c = 70$   $\mu\text{m}$ ) supports many longitudinal cavity modes in the transverse plane having a free spectral range  $\Delta\lambda \approx \lambda_0 / 2nd_c$ , where  $n$  is the core refractive index and  $\lambda_0$  is the lasing centre wavelength. The lasing spectrum was resolved into its modes, as shown in Fig. 3c, using an optical spectrum analyzer (ANDO AQ6317), and the 2-nm mode spacing (corresponding to a 68- $\mu\text{m}$  core diameter) is in good agreement with the expected value. The measured quality factor  $Q = \lambda_0 / \delta\lambda$  ( $\delta\lambda$  is the spectral width of one mode) of 640 is lower than theoretically expected. Possible reasons for this discrepancy are the losses arising from an imperfect cavity structure and the limited spectral resolution of the measurement setup.

The optical wave front emanating from the fiber laser has several unique characteristics that stem from the combination of the emission properties of the dye and the resonant cavity design. First, the emitted laser wave front has a dipole-like radiation pattern, shown in Fig. 4a. This result was obtained in two different ways. First the orientation of the pump polarization at the input to the fiber was rotated while a probe recorded the emitted intensity in the x-polarization at a fixed location along the y-axis. The measurement was then corroborated by physically rotating the probe around the surface of the fiber laser while keeping the pump polarization fixed in the x-direction. Upon comparing the radiation pattern to that of a bulk dye-doped copolymer excited with the same pump, we find the dipole-like radiation pattern is not as pronounced as in the fiber laser. These results can be understood by noting that the polarization of the dye fluorescence is determined mainly by the pump polarization and the relative orientation of the transition moments in the dye molecule for the absorption and emission transitions [12]. The polarized dye molecules that are aligned with the pump polarization contribute the most to the fluorescence. This may be confirmed by analyzing the dye emission with a linear polarizer rotated in the  $x$ - $z$  plane, normal to the direction of maximum emission ( $y$ -axis), with a fixed x-polarized pump, as shown in Fig. 4(b) (dotted line). The dipole radiation patterns of the dye molecules combine to result in the radiation pattern shown in Fig. 4(a) where the strongest radiation is in the direction orthogonal to the pump polarization and the fiber axis. Since fluorescence polarized parallel to the pump is stronger, cavity modes with this polarization have lower thresholds. Consequently, the fiber laser has an enhanced polarization component parallel to the pump as compared to that of the bulk dye emission (Fig. 4(b), solid line) and a more prominent dipole-like radiation pattern.

These interesting results suggest that the direction of the laser beam can be controlled remotely just by rotating the pump polarization.

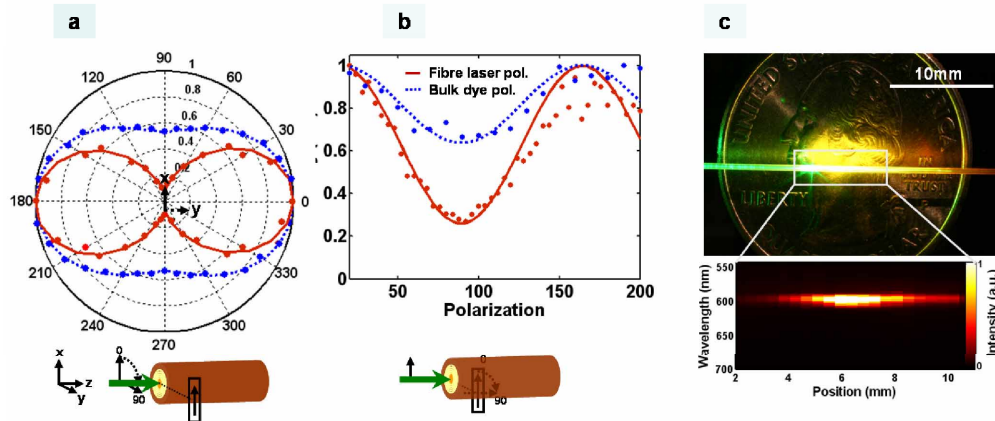


Fig. 4 Geometric dependence of the emission for an LDS698-doped PBG fiber laser. (a), Angular intensity pattern of the bulk dye and fiber laser emission at a fixed location along the  $y$ -axis measured by rotating the input polarization. This measurement is equivalent to fixing the pump polarization while measuring the emission intensity around the fiber. (b), Polarization of light emitted from bulk dye (dashed blue) and dye in a fiber cavity (red line) having a ratio of intensities in the  $x$ - and  $y$ -directions of 0.22 and 0.6, respectively, measured by fixing the pump polarization in the  $x$ -direction and recording the intensity as a function of polarizer rotation about the direction of maximum emission ( $y$ -axis). (c), Emission spectra from large core (200- $\mu\text{m}$ ) PBG fiber laser measured along the fiber axis at 10- $\mu\text{J}$  pump energy measured by scanning a probe fiber along the fiber side. The upper panel shows a photograph of the fiber showing laser light emitted from a spatially extended region along the fiber ( $\sim 5$  mm).

A second unique feature of this laser is that emission occurs over a spatially extended region by virtue of the extended surface area of the fiber resonator walls. This is in contrast to semiconductor [13, 14] and polymer [15] planar annular resonators in which the resonator thickness is on the order of the emission wavelength. Figure 4(c) shows the emission spectrum as a function of position along a large-core ( $d_c = 200 \mu\text{m}$ ) PBG fiber. By moving a probe along its axis we observed laser radiation extending along  $\sim 5$  mm of the fiber (measured at full-width-half-maximum). The upper panel of Fig. 4c shows a photograph of this operating laser. One may further increase the surface area from which laser light is emitted by optimizing dye concentration, core size, and PBG structure.

The dual action of the PBG structure as both a transverse laser cavity and a transmission waveguide is highlighted in Fig. 5(a). In this specific fiber, a short segment of Rhodamine 590 doped copolymer was introduced into a PBG fiber, leaving the rest of the core hollow. The photograph of the bent fiber displays both features: the hollow-core portion of the fiber transmits the pump light (green,  $\lambda = 532$  nm, top of the photograph), and the dye-doped portion emits orange-colored laser light ( $\lambda = 576$  nm).

Furthermore, the placement of dye-doped segments along a fiber can be carefully controlled. A demonstration that highlights the ability to finely tune segment size, location, and composition is shown in Fig. 5(b). A lasing display projects the letters "MIT" in two colors. All the lasing fibers contain copolymer segments doped with DCM (orange). Additionally, the "i"-fiber contains both DCM and LDS698 (red) demonstrating that more than one gain medium can be precisely placed in the same fiber. This specific display contains 12 dye-filled fibers that are pumped from both ends. The large segments contain less than 0.5  $\mu\text{l}$  of dye-doped polymer.

Finally, the use of dyes with fluorescence spectra that extend over the visible and near-IR wavelengths is made possible by simply scaling the PBG structure and hence shifting the band gap. Nine different dyes were inserted into separate fibers having band gaps matched to their

emission peaks. The lasing spectra of these fibers are displayed in Fig. 5(c), and photographs of three lasers are shown depicting bright blue, green and red laser light. Moreover, the fiber's photonic band gap is readily scalable from the UV [11] to the IR [8, 10].

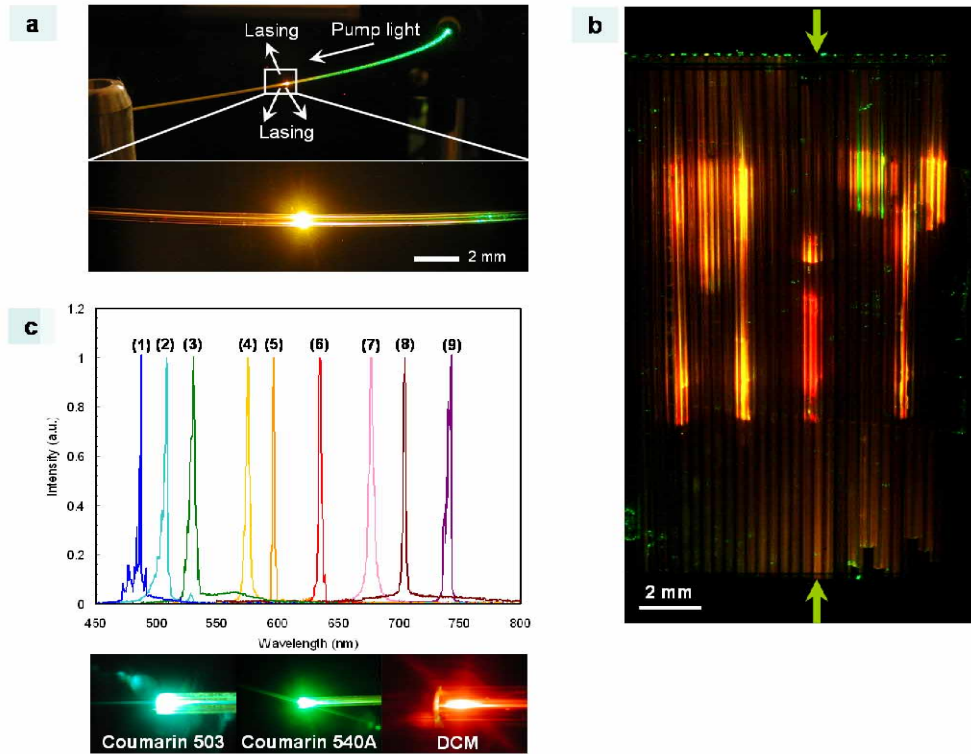


Fig. 5. (a). A photograph of an R590-doped PBG fiber showing the pump (532 nm, green) guided in the hollow-core PBG fiber. Lasing at 576 nm (orange) occurs in the R590-doped region. (b). Lasing "MIT" made out of 12 PBG fibers doped with DCM (orange) and LDS698 (red) that are simultaneously pumped in both directions. This display design illustrates the ability to finely tune dye location, size, and concentration. (c). Laser emission spectra from fibers doped with nine different dyes. The lasers producing emission spectra 1-3 are constructed using the same hollow-core PBG fibers having a fundamental reflection band gap at 500 nm, and were pumped at 355 nm. The fibers used to produce emission spectrum 4 has a fundamental reflection band gap at 600 nm, while those used for spectra 5-9 have a fundamental reflection band gap at 690nm, and all were pumped at 532 nm. Photographs of the organic dye-doped PBG fiber lasers showing the individual laser colors (blue, green and red) emitting from the fiber surface.

#### 4. Conclusions

This new polymer surface-emitting fiber laser offers unique control over the direction and polarization of the lasing wave front, is inherently wavelength scalable, and can be used for the remote delivery of radial laser emission. The ability to control the gain medium location, spatial extent, and concentration coupled with the fiber's mechanical flexibility paves the way for lasing textile fabrics or even 3D laser-light-emitting structures.

#### Acknowledgments

We thank S. D. Hart, Y. Kuriki, R. Dasari, M. Feld, J. Gardecki, F. Sorin, P. Bermel and JEOL Ltd. Japan for assistance. N. Orf gratefully acknowledges support through the National Defense Science and Engineering Graduate Fellowship program. This work was supported by US DOE DE-FG02-99ER45778 , DARPA/Christodoulou, the ARO through the ISN (contract

number DAAD-19-02-D-0002), the HEL-MURI through AFOSR (contract number Y77011) and the NSF ECS – 0123460. This work was also supported in part by the MRSEC Program of the National Science Foundation under award number DMR 02-13282. This work made use of the G.R. Harrison Spectroscopy Laboratory's laser facilities supported by the National Science Foundation (0111370-CHE).

### **Appendix A: Fiber Preparation**

The hollow-core PBG fiber preform was fabricated by thermal evaporation of an As<sub>2</sub>S<sub>3</sub> layer (5 μm) on both sides of a free-standing 8-μm-thick PEI film and the subsequent rolling of the coated film into a hollow multilayer tube. This hollow macroscopic preform with a thick protective outer layer of PEI was consolidated by heating under vacuum at ~ 260 °C and was then drawn in a fiber draw tower into hundreds of meters of fiber at ~ 305 °C. The SEM samples were prepared with JEOL Cross Section Polisher (CP) SM-09010 and the micrographs produced with JEOL JSM 7000F.

Mixed solutions of methyl methacrylate (MMA) and 2-hydroxyethyl methacrylate (HEMA) monomers containing t-butyl peroxide (tBP) or azobisisobutyronitrile (AIBN), n-butyl mercaptan, and organic dyes (0.05-0.5 wt%) were prepared and inserted into the hollow core PBG fibers. The fibers were placed in an oven at either 90 °C (tBP) or 60 °C (AIBN) for 20 hours for polymerization. All dyes were obtained from Exciton, Inc. The dyes used to produce the laser emissions shown in Fig. 5(a) are as follows: (1), 0.5 wt% coumarin 503; (2), 0.5 wt% coumarin 500; (3), 0.5 wt% coumarin 540A; (4), 0.1 wt% rhodamine 590; (5), 0.1 wt% DCM; (6), 0.1 wt% LD698; (7), oxazine 720; (8), 0.1 wt% LD700; (9), 0.1 wt% oxazine 725.

### **Appendix B: Optical Measurements**

The reflection spectra of the hollow-core fibers were measured using a xenon lamp (Oriel 68840-M). The light was collimated using a 5-cm focal-length lens, directed through a beam splitter, and focused onto the fiber outer surface using a ×10 microscope objective lens. The light reflected back from the multilayer structure was collimated by the objective lens and directed by the beam-splitter to a spectrometer (Ocean Optics HR2000CG-UV-NI) and then normalized with respect to the spectrum of the lamp.

The optical pump for the fiber lasers was a linearly polarized, pulsed Nd:YAG laser (Continuum Minilite II) with nominal pulse durations of 9 ns and repetition rate of 10 Hz. Both the second (532nm) and third (355nm) harmonics were utilized as pumps in accordance with the dye's fluorescence. The pump beam was spatially filtered by a 500-μm pinhole, a small percentage of the energy was directed away by a beam splitter to monitor the pump energy, a half-wavelength plate controlled the pump polarization, and a one-inch focal-length lens coupled the pump into the fiber core. The pump input energy was measured using an energy meter (Coherent PM1000, J4-09 and J3S-10). The energy of the resulting laser light emitted from the fiber laser was collected by an integrating sphere (Sphere Optics) and measured using the same energy meter with a high-pass filter mounted in front to eliminate any pump signal. The pump energy was adjusted using a variable optical attenuator. The emission spectra of the generated laser light were measured with the spectrometer after being collected by a 600-μm-diameter multimode fiber probe. The polarization measurements of both the bulk dye and the fiber were made using a linear sheet polarizer placed between the sample and the spectrometer.